



Structural studies and applications of water soluble (phenoxy)imine palladium(II) complexes as catalysts in biphasic methoxycarbonylation of 1-hexene

Saphan O. Akiri, Stephen O. Ojwach*

School of Chemistry and Physics, University of KwaZulu-Natal, Private Bag X01, Scottsville, Pietermaritzburg 3209, South Africa

ARTICLE INFO

Article history:

Received 14 January 2021

Revised 2 April 2021

Accepted 3 April 2021

Available online 15 April 2021

Keywords:

Palladium

Methoxycarbonylation

1-hexene

Biphasic

Recycling

ABSTRACT

Reactions of the ligands; sodium 4-hydroxy-3-((phenylimino)methyl)benzenesulfonate (**L1**), sodium 3-(((2,6-dimethylphenyl)imino)methyl)-4-hydroxybenzenesulfonate (**L2**) and sodium 3-(2,6-diisopropylphenyl)imino)methyl)-4-hydroxybenzenesulfonate (**L3**) with Pd(OAc)₂ afforded the respective palladium(II) complexes [Pd(**L1**)₂] (**PdL1**), [Pd(**L2**)₂] (**PdL2**) and [Pd(**L3**)₂] (**PdL3**). In addition, treatment of the non-water soluble ligands 2-((phenylimino)methyl)phenol (**L4**), 2-(((2,6-dimethylphenyl)imino)methyl)phenol (**L5**) and 2-(((2,6-diisopropylphenyl)imino)methyl)phenol (**L6**) with Pd(OAc)₂ gave the corresponding complexes [Pd(**L4**)₂] (**PdL4**), [Pd(**L5**)₂] (**PdL5**) and [Pd(**L6**)₂] (**PdL6**) in good yields. Solid state structures of complexes **PdL1** and **PdL4** established the formation of bis(chelated) square planar neutral compounds. All the complexes formed active catalysts in the methoxycarbonylation of 1-hexene, affording yields of up to 92% within 20 h and regioselectivity of 73% in favour of linear esters. The catalytic activity and selectivity of the complexes depended on the steric encumbrance around the coordination centre. The water soluble complexes displayed comparable catalytic behaviour to the non-water soluble systems. The complexes could be recycled five times with minimal changes in both the catalytic activities and regio-selectivity.

© 2021 Elsevier B.V. All rights reserved.

1. Introduction

The use of catalysts in industrial processes has triggered a significant increase in the production of various industrial and domestic products [1]. This mass production has on the other hand led to environmental concerns, which in turn has triggered the search and development of greener catalytic processes [2,3]. While the principles of green chemistry calls for catalysts which can be recycled and reused to minimize waste, the use of homogeneous catalysts in various industrial processes is still unavoidable [4]. This is mainly due to the selective nature of the homogeneous catalyst systems [5,6]. As such, various methods have been developed to make the homogeneous catalysts recyclable while, maintaining their selectivity. Some approaches that are currently being adopted include, the use of inorganic supports such as silica [7], magnetic supports [8], and polymer supports [9] and more recently the use of supported ionic liquid phases [10].

Another technology that has also not been left behind in this venture is the use of biphasic homogeneous catalyst systems [11].

Even though the most widely used combination of liquids in biphasic catalysis entails organic-aqueous biphasic system, other combinations include organic-organic biphasic, and of more recently, fluorinated solvents, and ionic liquids [12]. In addition to the ease of separation and recycling of biphasic systems, the use of water as a solvent is attractive due to its cheaper cost and non-toxicity [13,14]. While biphasic catalysts have been widely applied in hydroformylation reactions [15-17], Heck-coupling [18,19], Suzuki-Miyaura coupling [20,21], olefin oligomerization [22,23], and hydrogenation reactions [24-26] amongst others, there is limited reports of the same in the methoxycarbonylation reactions [27,28].

Methoxycarbonylation of olefins has gained interest due to the production of valuable ester products. Despite the fact that biphasic catalysis provides a suitable route for catalyst recycling and reuse, there are only a few reports on the use of water-soluble catalyst in methoxycarbonylation reactions. In addition, most of the reports entail biphasic catalysis in thermomorphic multicomponent solvents [29-31]. Even though, the thermomorphic multicomponent solvents systems are efficient for catalyst recycling, they mainly use hazardous solvents and can be relatively complex due to an elaborate selection of solvents. We have recently

* Corresponding author.

E-mail address: ojwach@ukzn.ac.za (S.O. Ojwach).

used homogeneous [32–37] and supported [38] catalyst systems in the methoxycarbonylation of olefins with varied catalytic activities and region-selectivities. In this current contribution, we report the design of water soluble palladium(II) complexes and their applications as biphasic catalysts in the methoxycarbonylation of 1-hexene. The non-water soluble palladium(II) analogues have also been studied for comparison purposes. Detailed structural studies of the palladium(II) complexes, influence of catalyst structure on catalytic behaviour and catalyst recycling have been investigated and are herein discussed.

2. Experimental section

2.1. Instrumentation and general materials

The reagents aniline (>99.5%), 2,6-dimethyl aniline (99%), 2,6-diisopropylaniline (90%), salicylaldehyde (98%), sodium carbonate, glacial acetic acid (>98%), palladium acetate (98%), sulphuric acid, 2-methoxyethylamine (98%) were purchased from Sigma-Aldrich and were used as received without further purification. Sodium 3-formyl-4-hydroxybenzenesulfonate was synthesised following a modified route of a previously reported procedure. All solvents purchased from Merck were of analytical grade and were dried before use. Toluene solvent was dried over sodium wire and benzophenone while methanol was dried and distilled by heating over magnesium metal activated with iodine. Dichloromethane was distilled using phosphorus pentoxide and stored in molecular sieves. Ligands **L4** and **L5** and their respective complexes **PdL4** and **PdL5**, having been reported before [39] were synthesised and used for comparison purposes with their water soluble analogues. ^1H NMR and ^{13}C NMR spectra were recorded on a Bruker Ultrashield 400 (^1H NMR 400 MHz, ^{13}C NMR 100 MHz) spectrometer in CDCl_3 and DMSO solution at room temperature. The chemical shift values (δ) were referenced to the residual proton and carbon signals at 7.24 and 77.0 ppm, respectively of the CDCl_3 NMR solvent and 2.50 and 39.52 ppm for DMSO. The infrared spectra were recorded on a Perkin-Elmer Spectrum 100 in the 4000–400 cm^{-1} range. Mass spectral analyses were carried out using LC premier Micro-mass, Elemental analyses were performed on a Thermal Scientific Flash 2000 whereas GC and GC-MS analyses was performed on a Varian CP-3800 and QP2010 respectively. X-ray data were recorded on a Bruker Apex Duo diffractometer equipped with an Oxford Instrument.

2.2. Single crystal X-ray crystallography

X-ray data for complexes were recorded on a Bruker Apex Duo diffractometer equipped with an Oxford Instruments Cryojet operating at 100(2) K and an Incoatec microsource operating at 30 W power. The data were collected with Mo $K\alpha$ ($\lambda = 0.71073 \text{ \AA}$) radiation at a crystal-to-detector distance of 50 mm. The following conditions were used for the data collection: omega and phi scans with exposures taken at 30 W X-ray power and 0.50° frame widths using APEX2[40]. The data were reduced with the programme SAINT [41] using outlier rejection, scan speed scaling, as well as standard Lorentz and polarisation correction factors. A SADABS semi-empirical multi-scan absorption correction was applied to the data. Direct methods, SHELXS-2014 and WinGX were used to solve all three structures. All non-hydrogen atoms were located in the difference density map and refined anisotropically with SHELXL-2014. All hydrogen atoms were included as idealised contributors in the least squares process. Their positions were calculated using a standard riding model with $\text{C-H}_{\text{aromatic}}$ distances of 0.93 \AA and $\text{U}_{\text{iso}} = 1.2 \text{ Ueq}$, $\text{C-H}_{\text{methylene}}$ distances of 0.99 \AA and $\text{U}_{\text{iso}} = 1.2 \text{ Ueq}$ and $\text{C-H}_{\text{methyl}}$ distances of 0.98 \AA and $\text{U}_{\text{iso}} = 1.5 \text{ Ueq}$.

2.3. Synthesis of water-soluble (phenoxy)imine palladium(II) complexes

2.3.1. Sodium

(E)-4-hydroxy-3-((phenylimino)methyl)benzenesulfonate palladium(II) (**PdL1**)

To a solution of $\text{Pd}(\text{OAc})_2$ (0.07 g, 0.31 mmol) in methanol (10 ml), was added a solution of **L1** (0.19 g, 0.62 mmol) in methanol (5 ml). The mixture was then stirred under nitrogen atmosphere for 24 h to give a yellow mixture, which was filtered and recrystallized using small portions of hexane to afford a bright yellow solid. Yield = 0.17 g (78%). ^1H NMR (400 MHz, DMSO): δ_{H} (ppm); 5.85 (d, 2H, $^3J_{\text{HH}} = 8.80 \text{ Hz}$, 6-PhO), 7.34–7.47 (m, 12H, Ar) 7.71 (d, 2H, $^4J_{\text{HH}} = 2.28 \text{ Hz}$, 3-PhO), 8.07 (s, 2H, H_{imine}). ^{13}C NMR (100 MHz, DMSO, δ ppm): 164.6 (CH-N), 164.2 (C-O), 149.2 (Ar-C), 136.2 (C-SO₃), 133.4 (Ar-C), 132.7 (Ar-C), 128.4 (Ar-C), 126.8 (Ar-C), 125.1 (Ar-C), 119.2 (Ar-C), 119.1 (Ar-C). IR $\nu_{\text{max}}/\text{cm}^{-1}$: $\nu_{(\text{C}=\text{N})} = 1605$, ESI-MS (m/z) = 678 [$\text{M}+\text{Na}$]⁺, 95%. Anal. Calc. for $\text{C}_{26}\text{H}_{18}\text{N}_2\text{Na}_2\text{O}_8\text{PdS}_2 \cdot 10\text{H}_2\text{O}$: C, 35.36; H, 4.34; N, 3.17. Found: C, 35.53; H, 4.08; N, 3.11.

2.3.2. Sodium (E)-3-(((2,6-dimethylphenyl)imino)methyl)benzenesulfonate palladium(II) (**PdL2**)

Complex **PdL2** was synthesized following the method outlined for **PdL1** using $\text{Pd}(\text{OAc})_2$ (0.05 g, 0.22 mmol) and **L2** (0.14 g, 0.44 mmol). Yield = 0.13 g (81%). ^1H NMR (400 MHz, DMSO): δ_{H} (ppm); 2.14 (s, 12H, Ar-CH₃), δ_{H} 5.78 (d, 2H, $^3J_{\text{HH}} = 8.8 \text{ Hz}$, Ar), 6.80 (d, 2H, $^3J_{\text{HH}} = 7.2 \text{ Hz}$, Ar), 7.34–7.47 (m, 6H, Ar) 7.65 (d, 2H, $^3J_{\text{HH}} = 2.0 \text{ Hz}$, Ar), 7.89 (s, 2H, H_{imine}). ^{13}C NMR (100 MHz, DMSO, δ ppm): 166.1 (CH-N), 162.9 (C-O), 149.1 (Ar-C), 146.1 (C-SO₃), 136.2 (Ar-C), 133.7 (Ar-C), 128.1 (Ar-C), 124.6 (Ar-C), 121.1 (Ar-C), 119.1 (Ar-C), 115.1 (Ar-C), 23.5 (C-H₃). IR $\nu_{\text{max}}/\text{cm}^{-1}$: $\nu_{(\text{C}=\text{N})} = 1607$, ESI-MS (m/z) = 780.99 [$\text{M}+\text{Na}$]⁺, 25%. Anal. Calc. for $\text{C}_{30}\text{H}_{26}\text{N}_2\text{Na}_2\text{O}_8\text{PdS}_2 \cdot 2\text{H}_2\text{O}$: C, 45.32; H, 3.80; N, 3.52. Found: C, 45.47; H, 3.70; N, 3.67.

2.3.3. Sodium

(E)-3-(((2,6-diisopropylphenyl)imino)methyl)benzenesulfonate (**PdL3**)

Compound **PdL3** was synthesized using the method described for **PdL1** using $\text{Pd}(\text{OAc})_2$ (0.05 g, 0.22 mmol) and **L3** (0.17 g, 0.44 mmol). Yield = 0.16 g (84%). ^1H NMR (400 MHz, DMSO): δ_{H} (ppm); 1.16 (d, 24H, $^3J_{\text{HH}} = 6.8 \text{ Hz}$ ipr), 3.05 (m, 4H, $\text{CH}_2\text{CH}_2\text{CH}$), δ_{H} 5.73 (d, 2H, $^3J_{\text{HH}} = 8.8 \text{ Hz}$, Ar), 6.80 (d, 2H, $^3J_{\text{HH}} = 7.2 \text{ Hz}$, Ar), 7.34–7.47 (m, 6H, Ar) 7.65 (d, 2H, $^3J_{\text{HH}} = 2.0 \text{ Hz}$), 7.95 (s, 2H, H_{imine}). ^{13}C NMR (100 MHz, DMSO, δ ppm): 165.4 (CH-N), 162.7 (C-O), 146.1 (Ar-C), 140.2 (C-SO₃), 134.4 (Ar-C), 133.7 (Ar-C), 128.1 (Ar-C), 124.6 (Ar-C), 123.5 (Ar-C), 120.7 (Ar-C), 119.2 (Ar-C), 31.2 (C-CH₃), 28.1 (C-H₃). IR $\nu_{\text{max}}/\text{cm}^{-1}$: $\nu_{(\text{C}=\text{N})} = 1604$. ESI-MS (m/z) = 893.20 [$\text{M}+\text{Na}$]⁺, 100%. Anal. Calc. for $\text{C}_{38}\text{H}_{42}\text{N}_2\text{Na}_2\text{O}_8\text{PdS}_2 \cdot 2\text{H}_2\text{O}$: C, 50.30; H, 5.11; N, 3.09. Found: C, 50.21; H, 4.95; N, 3.33.

2.3.4. (E)-2-(((2,6-diisopropylphenyl)imino)methyl)phenol palladium(II) (**PdL6**)

Complex **PdL6** was synthesized following the procedure used for **PdL4** using $\text{Pd}(\text{OAc})_2$ (0.17 g, 0.44 mmol) and **L6** (0.25 g, 0.88 mmol). Yield = 0.25 g (84%). ^1H NMR (400 MHz, CDCl_3): δ_{H} (ppm); 1.20 (d, 24 H, $^3J_{\text{HH}} = 5.4 \text{ Hz}$, ipr), 3.54 (m, 4H, $\text{CH}_2\text{CH}_2\text{CH}$) 6.01 (d, 2H, $^3J_{\text{HH}} = 6.72 \text{ Hz}$, 4-PhO), 6.46 (m, 2H, 4-PhO), 7.10 (m, 4H, 3,5-pH), 7.21 (d, 4H, $^3J_{\text{HH}} = 6.2 \text{ Hz}$, 5-PhO, 4Ph), 7.35 (t, 2H, $^3J_{\text{HH}} = 6.12 \text{ Hz}$ 3-PhO), (s, 2H, H_{imine}). ^{13}C NMR (100 MHz, CDCl_3 , δ ppm): 165.5 (CH-N), 162.7 (C-O), 144.8 (Ar-C), 142.4 (Ar-C), 134.8 (Ar-C), 134.3 (Ar-C), 126.6 (Ar-C), 122.8 (Ar-C) 120.8 (Ar-C), 119.5 (Ar-C), 114.2 (Ar-C), 28.8 (C(CH₃)₂) 24.3 (C-iPr): IR $\nu_{\text{max}}/\text{cm}^{-1}$: $\nu_{(\text{C}=\text{N})} = 1603$. Anal. Calc. for $\text{C}_{38}\text{H}_{44}\text{N}_2\text{O}_2\text{Pd}$: C, 68.41; H, 6.65; N, 4.20. Found: C, 68.36; H, 6.70; N, 4.26.

2.3.5. Reactions of PdL4 with PPh₃ [Pd(PPh₃)₂(L4)]⁺

To a solution of complex **PdL4** (0.10 g, 0.20 mmol) in chloroform (10.0 ml) was added NaBPh₄ (0.07 g, 0.20 mmol) and PPh₃ (0.11 g, 0.40 mmol) in chloroform (5.0 ml). The resulting yellow solution mixture was then stirred at room temperature for 24 h. The solution was filtered, concentrated in *vacuo* and hexane (10 ml) used to precipitate compound [Pd(PPh₃)₂(L4)]⁺ as a yellow solid. Yield = 0.12 g (80%). ¹H NMR (400 MHz, CDCl₃): δ_H (ppm); 6.13 (d, 1H, ³J_{HH} = 8.4 Hz, Ar), 6.54 (t, 1H, ³J_{HH} = 7.8 Hz, Ar), 6.83 (m, 1H, Ar), 7.05 (m, 2H, Ar), 7.23 (m, 6H, Ar), 7.33–7.50 (m, 30H, Ar, BPh₄), 7.52–7.68 (m, 8H, Ar), 7.71–7.78 (m, 10H, Ar) 7.84 (s, 1H, H_{imine}). ³¹P NMR (CDCl₃): δ 23.24 (s, 1P, PPh₃), 29.30 (s, 1P, PPh₃).

2.4. Methoxycarbonylation catalysis

2.4.1. General methoxycarbonylation experiment and analyses

The methoxycarbonylation catalytic reactions were performed in a stainless steel autoclave Parr reactor equipped with a temperature control unit, an internal cooling system and a sampling valve. In a typical experiment, **PdL4** (0.04 g, 0.08 mmol), HCl (0.050 mL), 1-hexene (2 mL, 16.00 mmol) and PPh₃ (0.13 g, 0.48 mmol) to give 0.5 mol% were placed in a Schlenk tube. A mixture of toluene (20 mL) and methanol (20 mL) were then added to dissolve them. The mixture was then introduced into the reactor and purged three times with CO, set at the required temperature and pressure and then the reaction stirred at 500 rpm. At the end of the reaction time, the reactor was cooled to room temperature and the excess CO vented off. Samples were drawn and filtered using micro-filter prior to GC analysis to determine the percentage yields of the products using ethylbenzene as an internal standard. GC-MS was used to determine the identity of the ester products, while the linear and branched esters were assigned using commercial linear methyl heptanoate standard sample. The GC analyses was carried out under the following conditions of: 25 m (1.2 mm film thickness) CP-Sil 19 capillary column, injector temperature 250 °C, oven program 50 °C for 4 min, rising to 200 °C at 20 °C/min and holding at 200 °C for 30 min, nitrogen carrier column gas 5 psi.

2.4.2. Procedure for biphasic methoxycarbonylation catalysis

The procedure in Section 2.4.1 was followed, except that water was used as a solvent in the biphasic catalysis. In a typical experiment, **PdL1** (0.056 g, 0.08 mmol), HCl (0.050 mL), 1-hexene (2 mL, 16.00 mmol) and PPh₃ (0.13 g, 0.48 mmol) to give 0.5 mol% were placed in a Schlenk tube. A mixture of methanol (18 mL) and water (1 mL), and toluene (20 mL) was then added to the mixture to dissolve them and create a biphasic medium. The mixture was introduced into the reactor and purged three times with CO, set at the required temperature and pressure and the reaction stirred at 500 rpm. At the end of the reaction time, the reactor was cooled to room temperature and the excess CO vented off. Samples were drawn and filtered using micro-filter prior to GC analysis to determine the percentage yields of the products using ethylbenzene as an internal standard.

2.4.3. Catalyst recycling experiments

The recycling of the water soluble complexes were performed by a simple decantation process. In a typical reaction using complex **PdL1**, by the end of a reaction, the reactor was allowed to cool to room temperature, excess CO gas vented and the reaction mixture transferred into a measuring cylinder. The mixture was allowed to stand to allow phase separation. The aqueous phase was then decanted from the organic phase and reintroduced into the reactor. Fresh 1-hexene substrate, PPh₃, HCl and toluene were then added and the reaction started for the next run. The analyses and quantification of the products were carried out using GC as outlined in Section 2.4.1.

3. Results and discussion

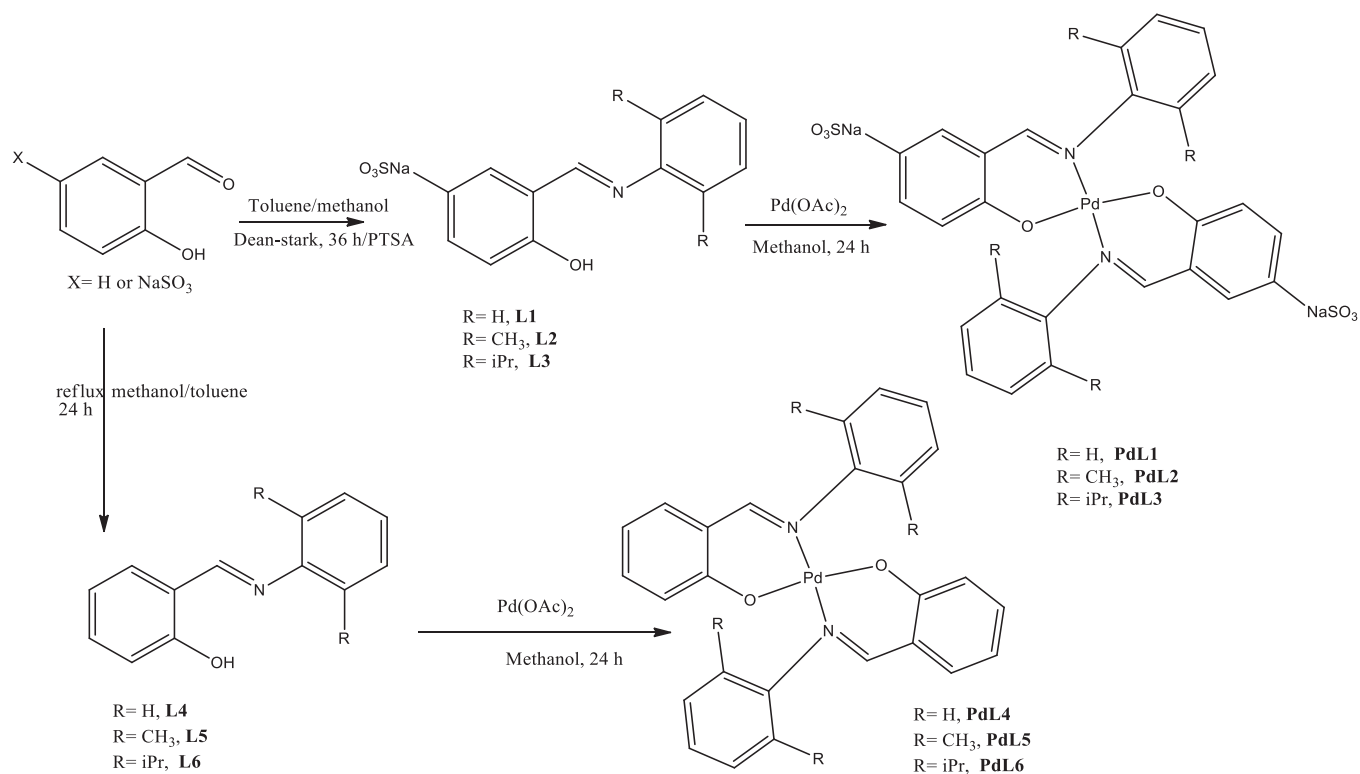
3.1. Synthesis of (phenoxy)imine ligands and their palladium(II) complexes

The sulfonated salicylaldehyde sodium 3-formyl-4-hydroxybenzenesulfonate synthon, was synthesized according to a modified reported procedure [42,43]. While the (phenoxy)imine sulfonate ligand **L1** was synthesised by refluxing using a Dean-Stark apparatus for 72 h, ligands **L2** and **L3** were synthesised under reflux using catalytic amounts of *para*-tolyl sulfonic acid for 48 h (Scheme 1). The non-water soluble (phenoxy)imine analogue **L4** was synthesized by stirring at room temperature, while compounds **L5** and **L6** were synthesized by reflux in toluene. All the new ligands were obtained in high yields of 84–88%. Reactions of ligands **L1–L6** with Pd(OAc)₂ acetate at room temperature afforded the respective complexes **PdL1–PdL6** in moderate to good yields (Scheme 1).

¹H NMR, ¹³C NMR and IR spectroscopies, mass spectrometry and elemental analyses were employed to identify all the new compounds. In the ¹H NMR spectra, the aldimine protons were observed between 8.52 to 9.02 ppm for ligands **L1–L6** (Figures S1–S12), consistent with previous reports [44,45]. The same imine proton was traced and used to infer the formation of the respective palladium(II) complexes. For instance, whereas the imine proton was observed at 9.02 ppm in ligand **L1**, the same proton shifted up field to 8.07 ppm in the respective complex **PdL1** (Figure S13). The FT-IR spectra of the ligands showed ν_(C=N) diagnostic peaks between 1605 and 1619 cm⁻¹ [45]. Upon complexation, general shifts in the absorption ranges of the imine bond were recorded. For instance, while the ν_(C=N) for **L1** was recorded at 1605 cm⁻¹, complex **PdL1** showed the same signal at 1615 cm⁻¹ (Figures S26 and S32). Another important feature of the IR spectra was the OH functionality. While the IR spectra of the ligands, showed the ν_(O-H) signals between 3 060 cm⁻¹ to 3 464 cm⁻¹, the respective complexes did not display this peak (Figures S26–S37), confirming deprotonation of the phenolic proton upon coordination to give the anionic ligands [36]. Mass spectrometry was further used to confirm the molecular masses of both the ligands and the respective complexes by comparing the experimental and theoretical isotopic mass distribution patterns (Figures S38 – S41). For instance, complex **PdL1** (M_w = 701.93) showed a molecular ion peak at 678.93 ([M-Na]⁺, consistent with the theoretical isotopic mass distribution (Figure S39). Similar observations were recorded for all the ligands and the respective palladium(II) complexes. The elemental analyses data supported the presence of two ligand units per palladium(II) atom and confirmed the purity of the bulk materials.

3.2. X-ray molecular structures of complexes PdL1 and PdL6

Single crystal suitable for X-ray analyses of complexes **PdL1** and **PdL6** were obtained by slow diffusion of hexane into their respective concentrated solutions in chloroform at room temperature. Table 1 shows the structural refinement parameters and crystallographic data, while Figs. 1 and 2 represent the molecular structures, selected bond angles and bond lengths of complexes **PdL1** and **PdL6** respectively. Complex **PdL1** consists of the Pd centre atom with two anionic bidentate ligand units to form a square planar coordination environment around the palladium(II) atom and the two O and two N donor atoms in a *trans*-configuration. The charge stabilization of the **PdL1** is accomplished by the cationic sodium-aqua complex. Only half of the anionic Pd complex, one hydrate molecule and a cationic sodium-aqua complex exist in the asymmetric unit (Fig. 1b). The Pd atom rests on an inversion centre; hence it has a site occupancy factor of 0.5. The oxidation state of Pd in the asymmetric unit, thus +1 whilst the



Scheme 1. Synthesis of water and non-water soluble (phenoxy)imine ligands and their respective palladium(II) complexes.

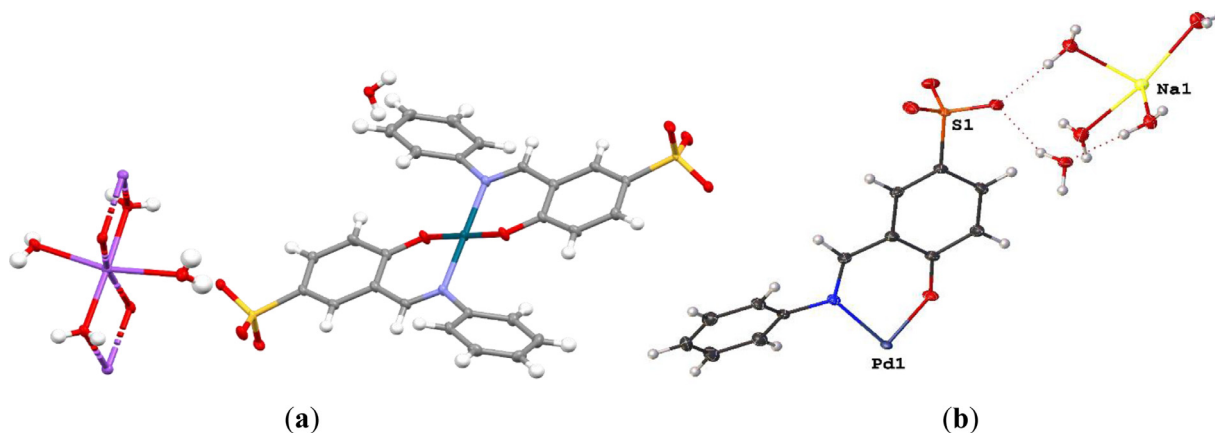


Fig. 1. (a) Molecular structure of **PdL1** with atom numbering Scheme. The displacement ellipsoids of atoms are shown at the 50% probability level. Selected bond lengths [Å]; Pd(1)-O(1), 1.9764(15); Pd(1)-N(1), 2.0282(19); Selected bond angles (°): O(1)-Pd(1)-O(1), 180.00(10); N(1)-Pd(1)-N(1), 180.00(10); O(1)-Pd(1)-N(1), 88.80(7); O(1)-Pd(1)-N(1)#1, 91.20(7). (b) Asymmetrical view of the unit showing only half of the anionic Pd complex, one hydrate molecule and the cationic sodium-aqua complex.

ligand bears a -2 charge from the phenolate (-1) and sulfonate (-1) moieties. Thus, the Pd complex is anionic (-1 overall charge) and is balanced by the cationic sodium-aqua complex ($+1$ overall charge). The complete complex **PdL1**, therefore forms a one dimensional, homometallic sodium-aqua coordination polymer upon the execution of the inversion symmetry operation. For every complete complex Pd(II), there are two Na-aqua complexes which form 1D coordination polymers via bridging aqua molecules. Complex **PdL6**, like **PdL1** has Pd atom centre with two anionic bidentate N[∧]O-donor (phenoxy)imine ligand units, to give a distorted square planar coordination geometry. The coordination chemistry of complexes **PdL1** and **PdL6** as established from the solid structures are in good agreement with the IR spectra (absence of O-H frequency).

The average Pd(1)-O(1) bond distances of 1.9764 (15)Å and 1.9776(15) Å for complexes **PdL1** and **PdL6** respectively are com-

parable. On the other hand, the average Pd-N_{imine} bond length for complex **PdL1** of 2.0282(19) Å is slightly longer than the Pd-N_{imine} bond distance of 2.013(15) Å for complex **PdL6** because of the inductive effects resulting from the iPr groups present in **PdL6**. The bond lengths exhibited by complexes **PdL1** and **PdL6** are comparable to similar reported compounds, where bond lengths for Pd(1)-O and Pd(1)-N_{imine} were recorded as 2.026 (16)Å and 2.067 (18)Å respectively [39]. Complex **PdL1** displays bite angles for O(1)-Pd(1)-N(1) and O(1)-Pd(1)-N(2) of 88.80(7)° and 91.20(7)° respectively, well within those recorded for complex **PdL6** of 92.14(6)° and 87.86(5)° respectively. This is consistent with minimal steric crowding around the Pd atoms in both complexes as the alkyl substituents are remotely located from the Pd centres. In general, complexes **PdL1** and **PdL6**, thus, adopt distorted square planar

Table 1

A Summary of the crystallographic data and structure refinement for complexes **PdL1** and **PdL6**.

Parameter	PdL1	PdL6
Empirical formula	C ₁₃ H ₁₉ N Na O ₉ Pd _{0.50} S	C ₃₈ H ₄₄ N ₂ O ₂ Pd
Formula weight	441.54	667.15
Temperature	100(2) K	100.02 K
Wavelength	0.71073 Å	0.71073 Å
Crystal system	Monoclinic	triclinic
Space group	P 21/c	P-1
Unit cell dimensions	19.9891(17) Å	7.9427(5) Å
a (Å)	6.8752(6) Å	10.1922(6) Å
b (Å)	13.5220(12) Å	11.1065(7) Å
c (Å)	90°	113.803(3)°
α (°)	103.238(2)°	96.819(3)°
β (°)	90°	97.945(3)°
γ (°)		
Volume	1808.9(3)	799.48
Z	4	1
Density (calculated)	1.621 Mg/m ³	1.386 Mg/m ³
Absorption coefficient	0.730 mm ⁻¹	0.616 mm ⁻¹
F(000)	904.0	348.0
Crystal size	0.260 × 0.140 × 0.020 mm ³	0.24 × 0.19 × 0.11 mm ³
Theta range for data collection	1.046 to 26.609°	4.084 to 58.026°

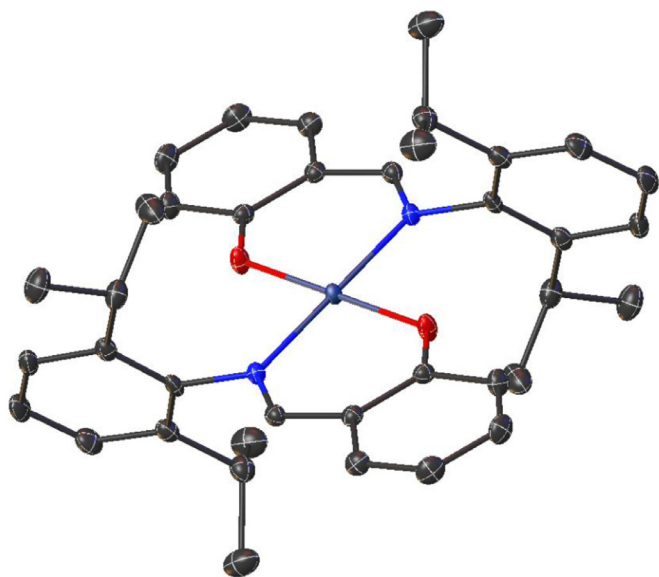


Fig. 2. Molecular structure of **PdL6** with atom numbering Scheme. The displacement ellipsoids of atoms are shown at the 50% probability level. Selected bond lengths [Å]: Pd(1)-O(1), 1.976(12); Pd(1)-O(2), 1.972(12); Pd(1)-N(1), 2.013(15); Pd(1)-N(2), 2.013(15); O(1)-C(6), 1.301(2). Selected bond angles (°): O(1)-Pd(1)-O(2), 180.0; N(2)-Pd(1)-N(1), 180.0; O(1)-Pd(1)-N(2), 87.86(5); O(1)-Pd(1)-N(1), 92.14(6).

coordination geometry, with the bite angles marginally deviating from typical square planar geometry of 90°

3.3. Methoxycarbonylation reactions catalysed by complexes **PdL1** and **PdL6**

3.3.1 Initial screening and optimization of the reaction conditions in the methoxycarbonylation of 1-hexene

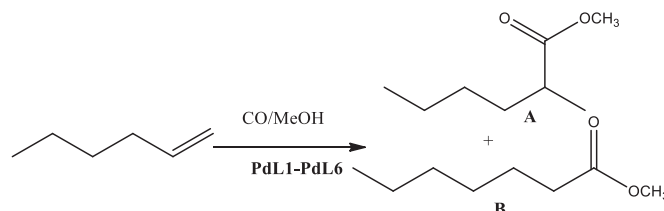
The initial screening of the complexes in the methoxycarbonylation reactions of 1-hexene was done using the non-water-soluble

Table 2

Initial screening and optimization of phosphine and acid promoter ratios in the methoxycarbonylation of 1-hexene using complex **PdL4**^a.

Entry	Pd: Acid	Pd:PPh ₃	Conv(%) ^b	Yield (%) ^b	B/L(%) ^c	TON ^d
1 ^e	1:10	0	0	0	–	–
2	1:10	1:2	55	52	36/64	104
3	1:10	1:4	69	68	31/69	136
4	1:10	1:6	85	83	30/70	166
5	1:10	1:8	80	78	27/73	156
6	1:20	1:6	92	92	30/70	184
7	1:5	1:6	46	43	30/70	86
8	1:30	1:6	71	68	31/69	136
9	1:40	1:6	44	43	29/71	86
10 ^f	1:20	1:6	44	41	29/71	82
11 g	1:20	1:6	70	67	30/70	134
12 ^h	1:20	–	–	–	–	–
13 ⁱ	1:20	1:6	9	7	30/70	20
14 ^j	1:20	1:6	23	20	32/68	80
15 ^k	1:20	1:6	84	82	34/66	164
16 ^l	1:20	1:6	72	71	30/70	142

^aReaction conditions: Pressure: 60 bar, temp: 90 °C, Solvent: methanol 20 mL and toluene 20 mL; [Pd]:[hexene] ratio; 1:200; time, 20 h; ^b% Conversions and yields determined from GC using ethylbenzene as internal standard. ^cMolar ratio between branched and linear esters calculated using linear methyl heptanoate commercial sample. ^dTON = (mol. prod/mol. Pd). ^e reaction done in the absence of PPh₃ ^f40 bar; ^g70 bar. ^hPd(OAc)₂/**L4**, ⁱPd(OAc)₂/**L4**/PPh₃; ^jPd(OAc)₂/PPh₃. ^kpara tolyl sulfonic acid (PTSA); ^lmethane sulfonic acid (MSA).



Scheme 2. Methoxycarbonylation of 1-hexene using complexes **PdL1-PdL6** as catalysts to give branched (**A**) and linear (**B**) esters.

complex **PdL4**. The ester products were identified and quantified using GC and GC-MS, by employing commercial methyl heptanoate (linear ester) sample and ethylbenzene as an internal standard (Figures S42 – S50). These allowed us to determine both the percentage conversions and yields as given in Tables 2-4. The TONs were calculated based on percentage yields. The comparable values in percentage yields and conversions suggest selectivity towards the ester products as depicted in Scheme 2. Typical reactions conditions of 1-hexene:HCl:PPh₃:Pd molar ratios of 200:10:2:1 (translating to 0.5 mol% of the Pd with respect to the substrate) were employed (Scheme 2 and Table 2). Under these conditions, complex **PdL4** afforded yields of 52% within 20 h and regioselectivity of 64% in favour of the linear ester (Table 2, entry 2). The role of the PPh₃ additive in the stabilization of the active species [46] was evident from the lack of catalytic activity reported in the absence of PPh₃ (Table 2, entry 1).

Informed by the bis(chelated) coordination chemistry of the complexes (Figs. 1 and 2), we envisioned that varying the amount of PPh₃ would have a major influence on the resultant catalytic activities of the complexes [47]. The use of acid promoters and phosphine additives in the methoxycarbonylation reactions is believed to generate and stabilize the active species respectively [47-49]. Thus, we varied the PPh₃/**PdL4** ratio from 2 to 8 (Table 2, entries 2 –5). We observed an increase in catalytic activity with increase in the amount of PPh₃, giving an optimum yield of 83% at PPh₃/**PdL4** ratio of 6 (Table 2, entry 4). Interestingly, a further increase of PPh₃/**PdL4** ratio to 8, was marked by a decline in percentage yield to 78% (Table 2, entry 5). Lower catalytic activities reported at higher PPh₃/**PdL4** may be associated with competition between the

PPh_3 ligand and the substrate for the active site [50]. Similar results were reported in the methoxycarbonylation of acetylene [51]. Separately, the lower catalytic activities observed at lower PPh_3/Pd ratios of 2 and 4 could be attributed to the bis(chelated) nature of the complexes, hence higher amounts of PPh_3 is required to displace the coordinated ligand units. Interestingly, the PPh_3/Pd ratio also influenced the regio-selectivity of the ester products. For example, $\text{PPh}_3/\text{PdL4}$ ratios of 2 and 8 afforded 64% and 73% of the linear esters respectively (Table 2, entries 2 vs 5). The higher linear ester products produced at higher $\text{PPh}_3/\text{PdL4}$ ratios may be assigned to increased steric hindrance from the bulky PPh_3 groups around the metal centre, thus favouring the less sterically demanding linear products [52].

Using the optimized $\text{PPh}_3/\text{PdL4}$ ratio of 6, we then varied the ratio of $\text{HCl}/\text{PdL4}$ between 5 and 40 (Table 2, entries 4 and 6 - 9). From Table 2, an optimum $\text{HCl}/\text{PdL4}$ ratio of 20 (92% yield) was realized. Increasing the amount of acid promoter is known to initiate efficient reactivation of palladium(0) formed under the reducing conditions [53]. Similarly, lower concentrations of the acid promoter has been shown to favour the formation of the less active palladium carbomethoxy intermediate [54]. In addition, excess acid is needed to achieve catalyst stability, since the acid promoter is consumed during the catalytic cycle. Apart from the acid promoter playing a role in the formation of active species, it is also required to shift the equilibrium from the inactive $\text{Pd}(0)$ species to the active intermediate species. However, further increase of the HCl concentration ($\text{HCl}/\text{Pd} > 20$) coincided with a decrease in catalytic activities (Table 2, entries 8 and 9). We also probed the behaviour of para-tolyl sulfonic acid (PTSA) and methanesulfonic acid (MSA) due to their mild natures as opposed to HCl in the methoxycarbonylation of olefins [51]. However, both PTSA and MSA displayed lower catalytic activities as compared to HCl . For example, using complex **PdL4**, conversions of 92%, 84% and 72% were realized for HCl , PTSA and MSA respectively (Table 2, entries, 6, 15 and 16). This is consistent with the dependence of catalytic activity on acid strengths, as previously reported by Zúñiga et al. [55].

To fully understand the role played by the coordinated ligands and isolated complexes in the generation of the active catalysts, we performed control experiments using $\text{Pd}(\text{OAc})_2/\text{L4}$ and $\text{Pd}(\text{OAc})_2/\text{L4}/\text{PPh}_3$ systems (Table 2, entries 12–14). The $\text{Pd}(\text{OAc})_2/\text{L4}$ and $\text{Pd}(\text{OAc})_2/\text{L4}/\text{PPh}_3$ systems gave much lower percentage yields of 7% and 20%, when compared to percentage yields of 92% displayed by complex **PdL4**/ PPh_3 catalyst system respectively (Table 2, entries 12–14 and 6). A similar observation has previously been made where the isolated complexes performed better than in-situ generated catalysts in methoxycarbonylation reactions [56]. From this data, it is conceivable that the coordinated ligands and the discrete metal complexes play a significant role in the generation of the active species in these methoxycarbonylation reactions.

Having established the optimum amounts of PPh_3 and HCl , we turned our attention to the effect of catalyst concentration by varying the 1-hexene/**PdL4** ratio from 1000 (0.1 mol%) to 100 (1 mol%) as shown in Fig. 3. The percentage yields were observed to increase with increase in catalyst loading. For example, at 1-hexene/**PdL4** ratio 500 (0.2 mol%) and 200 (0.5 mol%), percentage yields of 56%, and 92% were obtained respectively. However, a further of catalyst loading to 1.0 mol% resulted in a slight drop in percentage yield to 85% (Fig. 3). The decrease in catalyst activities at higher catalyst loading is not new and has been associated with catalyst aggregation [57,58]. Even though higher catalyst loadings led to higher percentage yields, it is important to note that, these were accompanied with lower TON values (Fig. 3). For instance, catalyst loadings of 0.2 mol% and 1.0 mol% recorded TON values of 280 (56%) and 80 (87%) respectively. The highest TON value of 292 (95%), was recorded at a lower catalyst loading of 0.25% (sub-

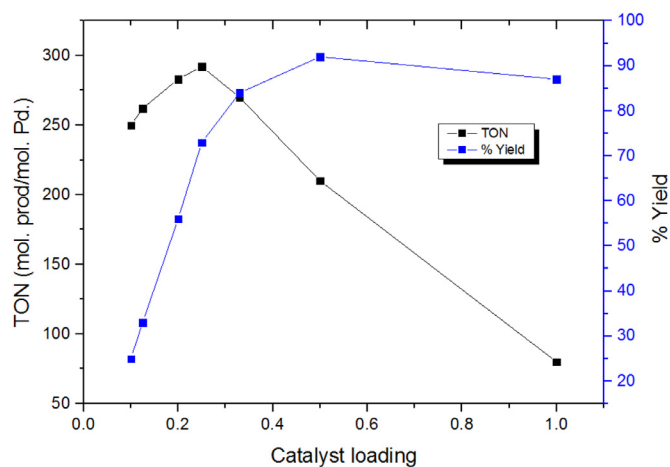


Fig. 3. A graphical plot showing the variations of TON and % yields with catalyst loading for complex **PdL4**. Catalyst loading varied from 0.1% (1:1000) to 1% (1:100).

strate/ $\text{Pd} = 400$). Thus, from this data, it is evident that higher catalyst loadings are not beneficial to the system. In terms of selectivity, the change in catalyst loading did not cause any substantial changes in regio-selectivity of the esters. For instance, catalyst loadings of 0.2 mol% and 0.5 mol% gave 71% and 70% of the linear esters respectively.

The influence of temperature was studied by changing the reaction temperatures from 50 °C to 90 °C (Figure S54). Expectedly reaction temperatures of 90 °C gave yields of 72%, while lower temperatures of 70 and 50 °C witnessed diminished yields of 59% and 40% (Figure S55) respectively [59]. On the other hand, elevated temperatures of 100 °C displayed resulted in lower yields of 65%, a trend that can be connected to partial catalyst decomposition to form palladium black [60] as observed from the reactor. On the other hand, temperature variations did not affect the regio-selectivity as values 68% to 71% of the linear products were obtained across all the temperature variations.

3.3.2. Investigation of the role of PPh_3 and HCl in the methoxycarbonylation reactions via *in situ* NMR techniques

Having observed significance dependence of catalytic activities of complex **PdL4** on the amounts of PPh_3 and HCl , our curiosity led us to try and understand the exact role these two play in regulating the catalytic activity. Thus *in situ* ^1H and ^{31}P NMR studies were employed to monitor the kinetics of formation and relative stabilities of possible active intermediates. The ^{31}P NMR experiment was performed using **PdL4**: PPh_3 ratios of 1:1, 1:2, 1:6 and 1:8 (Fig. 4). The ^{31}P NMR spectra showed multiple peaks within the region of 22 ppm to 33 ppm, indicating the formation of a number of $\text{Pd}-\text{PPh}_3$ adducts/intermediates [60–62]. Expectedly, the use of excess PPh_3 (PPh_3/Pd ratios of 6 and 8) gave signals at -5 ppm pointing to the presence of uncoordinated PPh_3 group. More significantly, the absence of the free PPh_3 signal at PPh_3/Pd ratio of 2 point to coordination of two PPh_3 units to Pd to give $[\text{Pd}(\text{PPh}_3)_2(\text{L4})]^+$ adduct, as a possible active species. Indeed, the lower yields reported at this PPh_3/Pd ratio of 2, point to insufficient stabilization of the active of the active species.

We also performed *in situ* ^1H NMR spectroscopy using **PdL4**/ PPh_3/HCl ratio of 1:8:20 by monitoring the changes in the ligand proton signals over a period of 9 h (Fig. 5). The main objective here was to establish if there is any hydrolysis of the imine group upon addition of HCl . Interestingly, no observable change to the imine signal at around 8.07 ppm was recorded over the 9 h period (Fig. 5). This was evident from the absence of the ligand **L1** (8.37 ppm) or aldehyde (9.80 ppm) signals. The invariable spectra

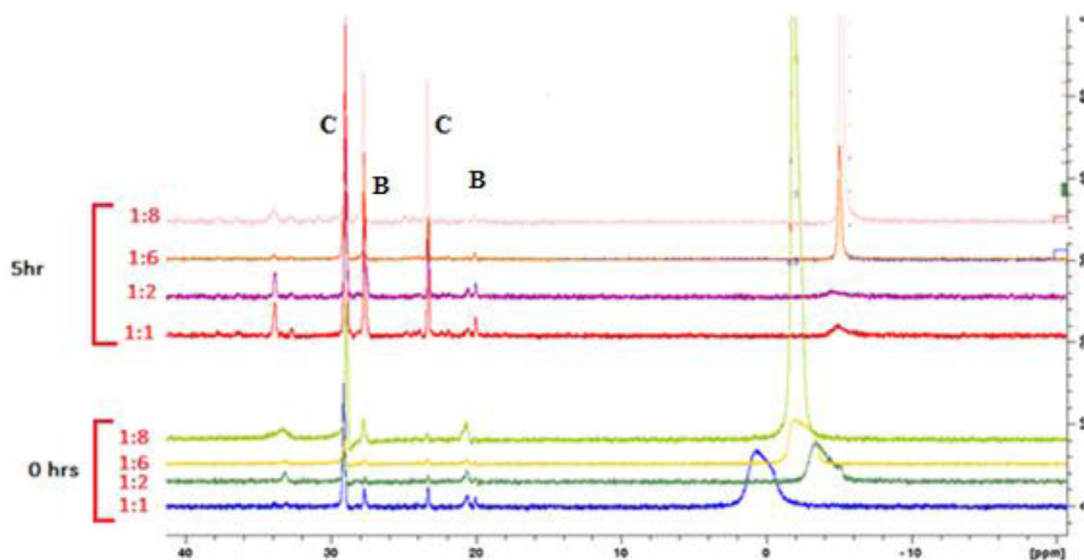


Fig. 4. ^{31}P NMR spectra showing various peaks for different concentrations of PPh_3 as a stabilizing agent using complex **PdL4**.

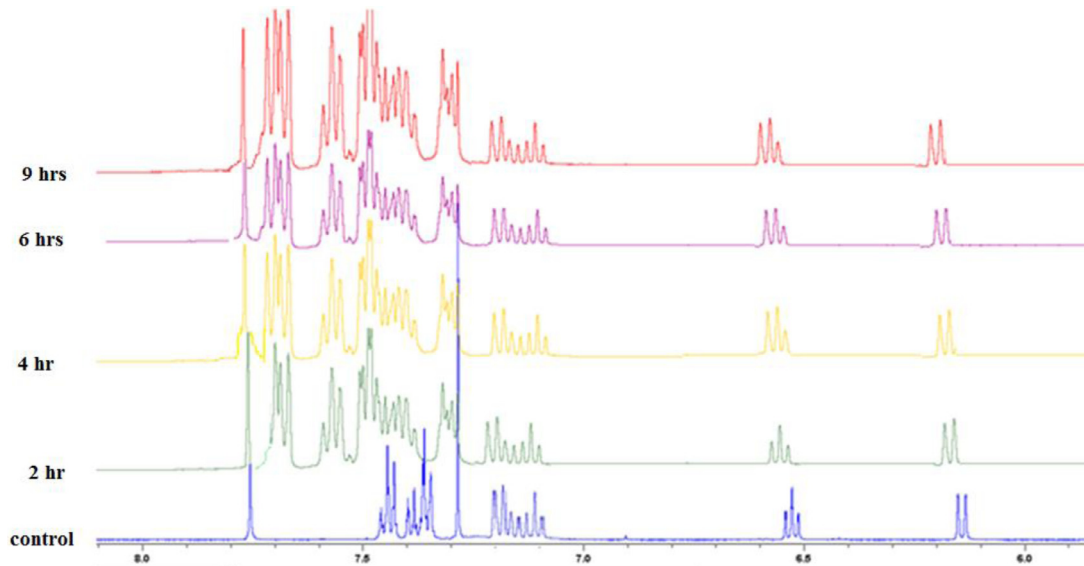
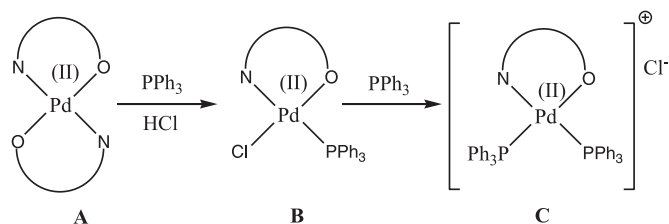


Fig. 5. ^1H NMR of complex **PdL4** in the presence of HCl and PPh_3 showing the stability of the complex **PdL4** in acid media over the 9 h period.

over the 9 h period thus pointed to the stability of complex **PdL4** under the experimental acidic conditions. The formation of the Pd-H group was expected, but unfortunately, no such signal at around 0 to -13 ppm was observed [63,64]. Instead, a signal at around 0.10 ppm was recorded, which at this stage, we are unable to unambiguously assign to the Pd-H species.

From the ^1H and ^{31}P NMR spectral studies, we are now in a position to propose possible stabilization and mechanistic routes in the generation of the active species for the methoxycarbonylation reaction using complex **PdL4** as depicted in **Scheme 3**. From **Scheme 3**, it is evident that the addition of HCl/PPh_3 mixture leads to complete dissociation of one ligand **L4** unit to give the mono PPh_3 intermediate $[\text{PdCl}(\text{L4})\text{PPh}_3]$ (**B**). This is derived from the signals observed in the ^{31}P NMR spectra at 21 ppm and 28 ppm, which corresponds to the mono-coordinated PPh_3 units either *trans* to the N- or O-donor atoms in **L4**. Similar palladium(II) complexes, bearing monodentate coordinated PPh_3 ligands, show the PPh_3 peaks at 32.49 and 23.28 respectively in their ^{31}P NMR spectra [62]. The formation of the bis-coordinated PPh_3 intermedi-



Scheme 3. Proposed activation and stabilization pathways of **PdL4** in the presence of PPh_3 and HCl .

ate $[\text{Pd}(\text{L4})(\text{PPh}_3)_2]^+$ (**C**), was evident from the observation of two signals at 23.8 ppm and 29.3 ppm (**Fig. 4**).

In attempts to establish the stability of the complexes under the catalytic conditions, we also obtained the ^1H and ^{31}P NMR spectra of the catalyst residue from the **PdL4**/ PPh_3 / HCl (1:8:20) system ran under the catalytic conditions of 60 bar of CO and 90°C (**Figures S56 & S58**). This was done by isolation of the spent catalyst af-

Table 3
Effects of complex structure on catalytic activity and regio-selectivity^a.

Entry	Catalyst	Conv.(%) ^b	Yield (%) ^b	B/L(%) ^c	TON ^d
1	PdL1	71	69	31/69	276
2	PdL2	66	64	29/71	256
3	PdL3	59	56	23/77	184
4	PdL4	73	72	30/70	288
5	PdL5	68	66	27/73	264
6	PdL6	60	59	23/77	236
7 ^e	PdL4	70	68	31/69	272
8 ^f	[Pd(PPh ₃) ₂ (L4)] ⁺	76	74	31/69	296
9 ^g	[Pd(PPh ₃) ₂ (L4)] ⁺	74	73	30/70	292
10 ^h	[Pd(PPh ₃) ₂ (L4)] ⁺	71	70	32/68	280

^a Reaction conditions: Solvent: methanol 20 mL and toluene 20 mL; [Pd]:[PPh₃]:[acid]:[hexene] ratio; 1:6:20:400; time, 20 h. ^bConversion and yield determined from GC using ethylbenzene as an internal standard and linear methyl heptanoate commercial sample. ^cMolar ratio between branched and linear ester. ^dTON = (mol. prod/mol. Pd). ^eHg drop experiment. ^{f,g,h} Pd:PPh₃ ratios of 1:6, 1:1, 1:0 respectively.

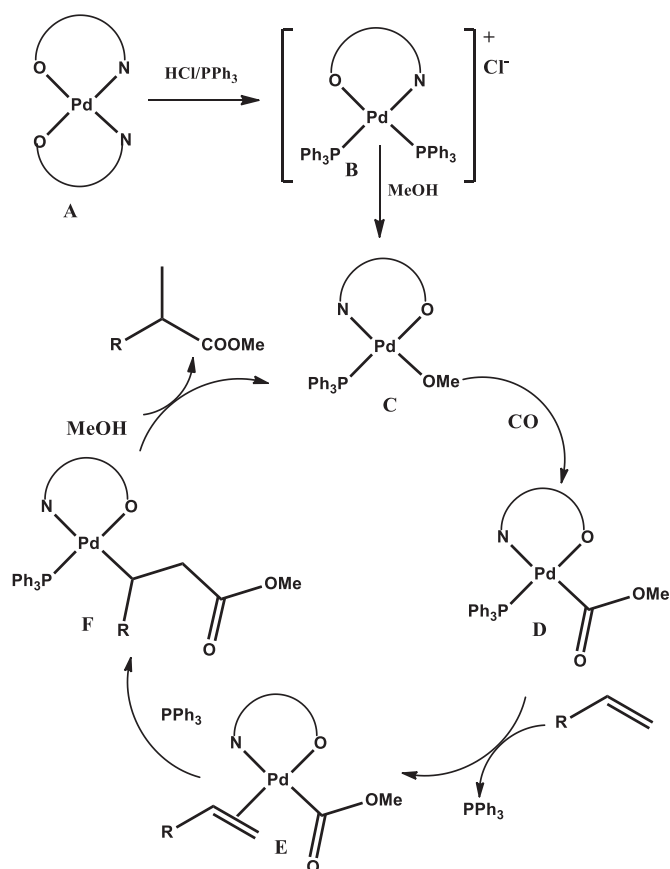
ter 20 h of reaction time. The ¹H NMR spectrum of the used catalyst was comparable to that of the original complex **PdL4**, with the imine proton being intact (Figure S56). Indeed, the ³¹P NMR spectra (Figures S57 and S58) of the spent catalyst were comparable to the spectra obtained at room temperature as well as the that of the original complex. Moreover, the two signals recorded at around 23 ppm and 30 ppm (Figure S58), do not compare to the one signal at around 24 ppm expected for the [Pd(PPh₃)₂Cl]₂ species [65]. This also points to the coordination of ligand **L4** to the metal atom to possibly give compound [Pd(PPh₃)₂(**L4**)]⁺ consistent with the proposed as shown in Scheme 3. This data therefore unequivocally established the stability of the active species and retention of the complex coordination environment, under the catalytic conditions.

We further attempted to confirm the presence of [Pd(PPh₃)₂(**L4**)]⁺ intermediate (Scheme 3) as if it is the active species. This was done by isolation of the product of the reactions of two equivalent of PPh₃ with **PdL4** (section 4.3.9). Both the ¹H NMR and ³¹P NMR spectra (Figures S59 & 60) of the isolated residue pointed to the formation of [Pd(PPh₃)₂(**L4**)]⁺ compound. For example, all the aromatic protons (60) were accountable for in the ¹H NMR spectrum (Figure S59), confirming the presence of one ligand **L4** unit and two coordinated PPh₃ ligands in the Pd coordination sphere. This was augmented by the signals at 23.2 ppm and 29.3 ppm in the ³¹P NMR spectrum (Figure S60). Even though a ²J_(P-P) coupling was expected, ³¹P NMR spectrum of [Pd(PPh₃)₂(**L4**)]⁺ did not exhibit such coupling/splitting as the two PPh₃ groups appeared as singlets. The observation could be attributed to a rapid ligand exchange resulting in exchange-averaged resonances [66].

Complex **PdL4a** was then used as a catalyst in the presence and absence of PPh₃ additive (Table 3, entries 8–10). Interestingly, the catalyst [Pd(PPh₃)₂(**L4**)]⁺ showed comparable catalytic activities to complex **PdL4**. For instance, percentage yields of 72% and 74% were recorded for complexes **PdL4** and [Pd(PPh₃)₂(**L4**)]⁺ respectively (Table 3, entries 4 vs 8). Most significantly, complex [Pd(PPh₃)₂(**L4**)]⁺ did not require the addition of PPh₃, as appreciable yields of 70% was recorded in the absence of PPh₃ (Table 3, entry 10). These observations therefore implicated [Pd(PPh₃)₂(**L4**)]⁺ intermediate as the possible active species in these reactions.

3.3.2.1. Proposed mechanism of the methoxycarbonylation of styrene.

From the NMR studies and the roles of PPh₃ and HCl as given in Scheme 3, we can thus propose a plausible mechanistic methoxycarbonylation route given in Scheme 4. Even though palladium(II) catalysed methoxycarbonylation reactions can proceed through two distinct routes (hydride and carbomethoxy) [67], the hydride mechanism has been proven to be favoured [68–71]. In this case,



Scheme 4. Proposed carbomethoxy mechanistic for the methoxycarbonylation of styrene catalysed by complexes 1–6.

no Pd-hydride species was captured in the ¹H NMR studies, hence we can hypothesize that the carbomethoxy route may be operational (Scheme 4). The catalytic cycle is triggered by ligand dissociation from the bis(chelated) complex **A**, to allow the coordination of the PPh₃ giving the [Pd(L)(PPh₃)₂]Cl (**B**). This is followed by formation of the methoxy species **C** in the presence of methanol solvent. The ester species **D** is then formed by migratory insertion of CO substrate to the Pd-OMe bond. Coordination of the olefin substrate to the carbomethoxy species **D**, via displacement of the coordinated PPh₃ ligand, results in the π -bonded olefin complex **E**. Migratory insertion of the sigma-bonded carbomethoxy group into the Pd-olefin bond, results in the ester product formation and recoordination of the PPh₃ ligand to give intermediate **F**. Methanolysis of the species **F**, finally leads to the elimination of the ester product and regeneration of the Pd-OMe species **C**.

3.3.3. Effect of complex structure on methoxycarbonylation reactions

Upon establishing the optimum conditions of temperature, catalyst loading, acid and phosphine additives for the methoxycarbonylation reactions using complex **PdL4**, we then investigated the comparative catalytic performance of the six complexes as shown in Table 3. From the data in Table 3, we observed some dependence of catalytic activities on the steric parameters of the complexes. For example, the unsubstituted complex **PdL1** recorded yields of 69% while the isopropyl substituted complex **PdL3**, afforded yields of 56% (Table 3, entries 1 vs 3). This trend can be assigned to the increased steric encumbrance around the metal atom, thus hindering substrate coordination. This an observation mirrors those of Harmon et al., where sterically hindered ruthenium(III) complex showed reduced catalytic activities [72]. Interestingly, the water-soluble complexes **PdL1–PdL3** showed compa-

Table 4
Biphasic catalysis and aqueous phase modification^a.

Entry	Complex	Volume of Water (mL)	Conv(%) ^b	Yield% ^b	B/L(%) ^c	TON ^d
1	PdL1	0	71	70	31/69	280
2	PdL1	1(5%)	68	67	30/70	268
3	PdL1	2 (10%)	65	63	32/68	252
4	PdL1	3(15%)	60	58	30/70	232
5	PdL1	4(20%)	51	50	31/69	200
6	PdL1	6(30%)	25	22	29/71	88
7	PdL1	8(40%)	Trace	–	–	–
8	PdL2	1(5%)	64	62	26/74	248
9	PdL3	1(5%)	55	52	22/78	208
10 ^e	PdL1	1(5%)	66	64	31/69	256

^aReaction conditions: Pressure: 60 bar, temp: 90 °C, Solvent: methanol (varying volumes) and toluene 20 mL;%water in the aqueous phase. [Pd]:[PPH₃]:[acid]:[hexene] ratio: 1:6:20:400; time, 20 h; ^b%Conversions and yields determined from GC using ethylbenzene as internal standard and linear methyl heptanoate commercial sample. ^cMolar ratio between branched and linear ester. ^dTON = (mol. prod/mol. Pd h⁻¹). ^eHg drop experiment.

rable catalytic activities to their respective non-water soluble counterparts **PdL4–PdL6** (Table 3). For instance, while the water-soluble **PdL1** displayed yields 69%, the corresponding complex **PdL4** exhibited yields of 72% (Table 3, entries 1 vs 4). This showed that incorporation of the water-soluble motif did not compromise the catalytic activities of the complexes, hence a major achievement in the design of separable catalyst systems.

The activities observed for the non-water soluble complexes compare well with similar systems reported in literature. While some systems performed better in methoxycarbonylation [46], others reported lower activities. For instance, 2-(diphenylphosphinoamino)pyridine palladium complexes by Aguirre et al. reported showed TONs of 340, compared to our TONs of 276 in the methoxycarbonylation of 1-hexene. On the other hand, palladium complexes of naphthyl(diphenyl)phosphines, benzimidazolylemethylamine palladium complexes and mixed N[^]N[^]X (X = O and S) ligands reported lower TONs of 190 in the methoxycarbonylation of 1-hexene.

In terms of regio-selectivity, the formation of either the linear or branched ester products was also affected by the steric crowding around the complexes. For instance, while the unsubstituted catalyst **PdL1** gave 69% of the linear isomer, the more sterically demanding isopropyl complex **PdL3** produced 77% of the linear ester. Increased steric bulk around the coordination centre is known to favour 1,2 olefin insertion, hence preference to the less bulky linear products [52]. The increase in linear products with steric crowding of the catalyst supports the operation of a carbomethoxy mechanism as discussed in Scheme 2 [52,53]. More importantly, the regio-selectivity of the water-soluble complexes were similar to those of the non-water analogues. For example, complexes **PdL1** and **PdL4** gave 69% and 70% of the linear esters respectively (Table 3, entries 1 vs 4). This clearly shows that incorporation of the water-soluble motif on the ligand backbone did not alter the selectivity of the resultant catalysts.

3.3.4. Biphasic methoxycarbonylation reactions using water soluble complexes **PdL1** – **PdL3**

Even though the use of water-soluble complexes in methoxycarbonylation of olefins is considered environmentally benign, to date, there are few reports on such catalysts [29–31]. Herein, we have carried out the methoxycarbonylation of 1-hexene under biphasic conditions (water/toluene/methanol system) using the water soluble complexes **PdL1** – **PdL3**. First, we established the best solvent ratio by varying the amount of water solvent using complex **PdL1** (Table 4). While keeping the volume of the organic phase (toluene) constant at 20 mL, we varied the amounts of water (0–40%) and methanol to give a total volume of 20 mL of the aqueous phase at

any given time. It was noted that addition of 1 mL of water (5% of the aqueous phase) to the toluene/methanol system gave yields of 67%, in comparison to 70% recorded in the pure toluene/methanol solvent (Table 4, entries 1 vs 2). However, under these conditions, phase separation required up to 10 h (Figure S61). Increasing the water content to 2 mL (10%) resulted in a slight decrease in percentage yield to 63%, but significantly, phase separation occurred within 2 h. A further increase in the water contents had detrimental effects, giving only 22% percentage yields at 6 mL (30%) of water content, while no activity was observed upon addition of 8 mL (40%) of water (Table 4, entries 4–7 and Figure S62). This phenomenon has been observed by Schmidt et al., where the use of 50% of water in the aqueous phase led to a complete loss of catalytic activity [27]. The lower yields observed with increased water has been attributed to reduced solubility of 1-hexene and CO in the aqueous phase [27], since CO has a low solubility value of 0.03 mol/L in pure water, compared to solubility of 0.28 mol/L in pure methanol [73]. As expected, complete decomposition of the catalyst was observed at 40% water, as deduced from extensive formation of Pd(0) black in this experiment.

The product distribution however, remained unaltered as 68% –71% of the linear esters was observed. Surprisingly, no carboxylic acid products (Figure S46) were observed even with increased water content through hydroxycarbonylation as has been observed in other related contributions [74]. We thus applied the conditions which led to higher catalytic activities to the water soluble complexes **PdL2** and **PdL3** in the methoxycarbonylation of 1-hexene (Table 3, entries 8 and 9). Consistent with the homogeneous trends, the catalytic activities of the complexes followed the order of **PdL1** > **PdL2** > **PdL3**. It is important to note that the catalytic activities recorded in both the homogeneous and biphasic media were comparable. For example, complex **PdL1** gave yield of 70% and 67% under homogeneous and biphasic conditions respectively (Tables 3 and 4).

3.3.5 Catalyst recycling studies

The promising performance of the water soluble complexes **PdL1** – **PdL3** under biphasic conditions, prompted us to investigate their potential to be recycled in the methoxycarbonylation of 1-hexene. This was achieved by carrying out the reactions for 24 h, followed by separation of the organic phase from aqueous layer and reusing the aqueous phase containing the catalyst (Fig. 6). From the Fig. 6, it was evident that the complexes significantly retained their catalytic activities in the five cycles investigated, recording drops of between 11% –15%. For example, catalyst **PdL1** recorded yields of 93% and 79% in the first and fifth runs respectively. It is worth noting that the selectivity of the complexes

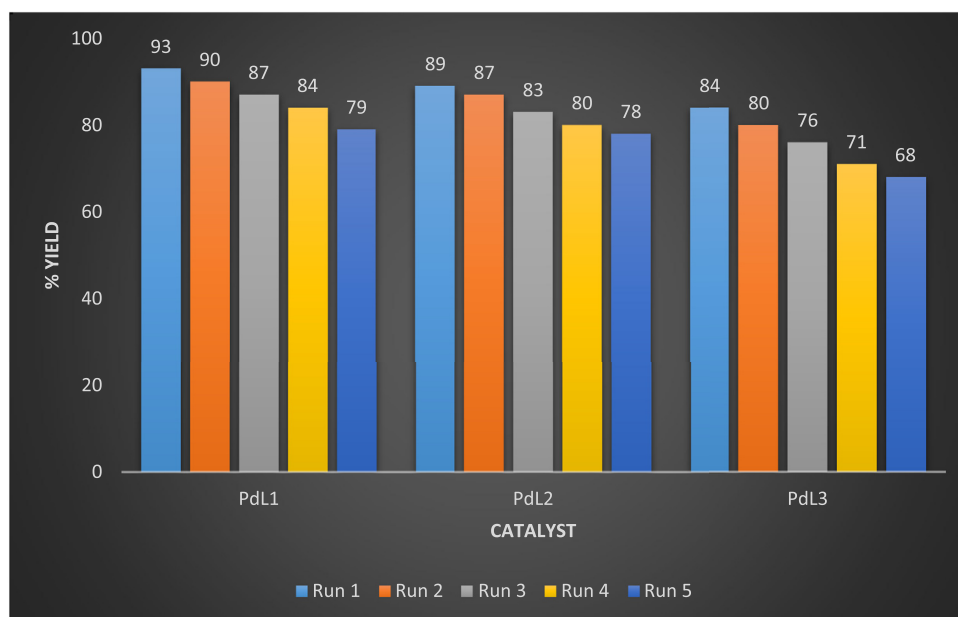


Fig. 6. A graph showing catalytic activities of complexes **PdL1- PdL3** with % yields of subsequent cycles in the methoxycarbonylation of 1-hexene. Reaction conditions: time, 24 h; CO: 60 bar; temp, 90 °C; solvent, toluene (20 mL), methanol (18 mL), water (2 mL).

was not affected in the recycling experiments. For instance, complex **PdL1** afforded regio-selectivities towards the linear esters of 70% and 71% in the first and fifth cycles.

The observed decline in catalytic activities may be associated with leaching of the catalyst into the organic phase and or catalytic degradation in subsequent cycles [75,76]. In order to ventilate if leaching may be responsible for the observed decline in catalytic activities, we performed hot filtration tests using complex **PdL1**. This was accomplished by running the reaction for 12 h, followed by separation of the aqueous phase containing the active catalyst. The organic phase, was then reintroduced into the reactor with fresh methanol and the reaction allowed to run for a further 24 h to mimic the recycling experiments. While in the first 12 h, percentage yields of 36% was reported, the next 12 h (24 h total time) only realized percentage yields of 39%. This translates to an increase of 3% in the next 12 h, suggesting the presence of some traces of the active species in the organic phase. In addition, this 3% increase is comparable to a drop in catalytic from 95% to 90% in the first and second cycles. Thus leaching of the active species may be implicated in the loss of catalytic activities in the recycling experiments. In an effort to gain some insight into the true nature of the active species (possible formation of any Pd(0) active nanoparticles), centrifugation of the **PdL1** catalyst was carried out after 10 h of reaction time. The supernatant liquid was then decanted off and reintroduced into the reactor, and the reaction run for a further 10 h. An increase in percentage yield from 27% within the first 10 h to 66% (original yield was 67%, Table 4, entry 1) in the next 10 h, points to a purely homogeneous system without the formation of any active Pd(0) nanoparticles. We also carried out Hg(0) experiments to further establish the homogeneity of the active species using the water soluble and non-water soluble catalysts (**PdL1** and **PdL4**). While the control reactions gave percentage yields of 68% and 72%, the experiments carried out using 5 drops of Hg(0) recorded percentage yields of 64% and 70% for complexes **PdL1** and **PdL4** respectively (Table 3, entry 7 and Table 4, entry 10). These comparable catalytic activities support the absence of any active Pd(0) nanoparticles and thus the homogeneous nature of the active species, consistent with the data obtained in the hot filtration and centrifugation experiments.

4. Conclusions

In summary water-soluble and non-water-soluble palladium(II) complexes anchored on anionic N^oO (phenoxy)imine ligands have been synthesized and structurally characterized. The solid structures of the complexes establish the existence of two anionic bidentate ligand units to form distorted square planar complexes. All the palladium(II) complexes formed active catalysts in the methoxycarbonylation of 1-hexene in favour of formation of linear esters. Both the catalytic activity and regioselectivity of the catalysts appear to be controlled by steric encumbrance around the palladium(II) atom. The water-soluble complexes exhibited comparable catalytic activities and regio-selectivities to their homogeneous systems. Under biphasic conditions, the complexes could be recycled up to five times with minimum loss of catalytic activity, but without any change in regio-selectivity. Hot filtration, centrifugation and Hg(0) drop experiments pointed to the homogeneous nature of the active species under biphasic conditions.

Declaration of Competing Interest

The authors declare that they have no known competing financial interests or personal relationships that could have appeared to influence the work reported in this paper.

Acknowledgements

The authors thank the DST-NRF (South Africa) Centre of Excellence in Catalysis (c*change) and the University of KwaZulu-Natal for financial support.

Supplementary materials

Supplementary material associated with this article can be found, in the online version, at [doi:10.1016/j.jorganchem.2021.121812](https://doi.org/10.1016/j.jorganchem.2021.121812).

References

- [1] I. Delidovich, R. Palkovits, Catalytic versus stoichiometric reagents as a key concept for Green Chemistry, *Green Chem* 18 (3) (2016) 590–593.

- [2] P. Anastas, N. Eghbali, Green chemistry: principles and practice, *Chem. Soc. Rev.* 39 (1) (2010) 301–312.
- [3] R.A. Sheldon, Fundamentals of green chemistry: efficiency in reaction design, *Chem. Soc. Rev.* 41 (4) (2012) 1437–1451.
- [4] J. Hagen, Industrial catalysis: a Practical Approach, John Wiley & Sons, 2015.
- [5] C. Copéret, F. Allouche, K.W. Chan, M.P. Conley, M.F. Delley, A. Fedorov, I.B. Moroz, V. Mougel, M. Pucino, K. Searles, Bridging the gap between Industrial and Well-defined supported catalysts, *Angew. Chem. Int. Ed.* 57 (22) (2018) 6398–6440.
- [6] J. Pritchard, G.A. Filonenko, R. van Putten, E.J. Hensen, E.A. Pidko, Heterogeneous and homogeneous catalysis for the hydrogenation of carboxylic acid derivatives: history, advances and future directions, *Chem. Soc. Rev.* 44 (11) (2015) 3808–3833.
- [7] E.A. Karakanov, A.V. Zolotukhina, A.O. Ivanov, A.L. Maximov, Dendrimer-encapsulated Pd nanoparticles, immobilized in silica pores, as catalysts for selective hydrogenation of unsaturated compounds, *ChemistryOpen* 8 (3) (2019) 358.
- [8] A. Vavasori, S. Bravo, F. Pasinato, N. Kudaibergenov, L. Pietrobbon, L. Ronchini, Supported palladium metal as heterogeneous catalyst precursor for the methoxycarbonylation of cyclohexene, *Mol. Catal.* 484 (2020) 110742.
- [9] Y. Wan, Z. Chen, D. Liu, Y. Lei, Palladium nanoparticles supported on Triphenylphosphine-Functionalized Porous Polymer as an active and recyclable Catalyst for the carbonylation of chloroacetates, *Catalysts* 8 (12) (2018) 586.
- [10] S.G. Khokarale, E.J. Garcia-Suarez, R. Fehrmann, A. Rüsager, Highly selective continuous gas-phase methoxycarbonylation of ethylene with supported ionic liquid phase (SILP) catalysts, *ChemCatChem* 9 (10) (2017) 1824–1829.
- [11] M. Illner, M. Schmidt, T. Pogrzeba, C. Urban, E. Esche, R. Schomäcker, J.-U. Repke, Palladium-Catalyzed methoxycarbonylation of 1-dodecene in a two-phase system: the path toward a continuous process, *Ind. Eng. Chem. Res.* 57 (27) (2018) 8884–8894.
- [12] F. Joo, Biphase Catalysis-Homogeneous. *Encyclopedia of Catalysis*, John Wiley & Sons, Inc, 2012.
- [13] T. Welton, Solvents and sustainable chemistry, *Proc. R. Soc. Lond. Ser. A Math. Phys. Eng. Sci.* 471 (2183) (2015) 20150502.
- [14] K.H. Shaughnessy, Hydrophilic ligands and their application in aqueous-phase metal-catalyzed reactions, *Chem. Rev.* 109 (2) (2009) 643–710.
- [15] K. Künnemann, L. Schurm, D. Lange, T. Seidensticker, S. Tilloy, E. Monflier, D. Vogt, J. Dreimann, Continuous hydroformylation of 1-decene in an aqueous biphasic system enabled by methylated cyclodextrins, *Green Chem.* 22 (12) (2020) 3809–3819.
- [16] J. Bianga, N. Herrmann, L. Schurm, T. Gaide, J.M. Dreimann, D. Vogt, T. Seidensticker, Improvement of productivity for aqueous biphasic hydroformylation of methyl 10-undecenoate: a detailed phase investigation, *Eur. J. Lipid Sci. Technol.* 122 (1) (2020) 1900317.
- [17] A. Cocq, H. Bricout, F. Djedaini-Pilard, S. Tilloy, E. Monflier, Rhodium-Catalyzed aqueous biphasic olefin hydroformylation promoted by amphiphilic cyclodextrins, *Catalysts* 10 (1) (2020) 56.
- [18] S. Jagtap, R. Deshpande, True water soluble palladium-catalyzed Heck reactions in aqueous-organic biphasic media, *Tetrahedron Lett.* 54 (21) (2013) 2733–2736.
- [19] S.V. Jagtap, R.M. Deshpande, PdCl₂ (bipy) complex—An efficient catalyst for Heck reaction in glycol-organic biphasic medium, *Catal. Today* 131 (1–4) (2008) 353–359.
- [20] H.B. Wang, Y.-L. Hu, D.-J. Li, Facile and efficient Suzuki–Miyaura coupling reaction of aryl halides catalyzed by Pd₂(dba)₃ in ionic liquid/supercritical carbon dioxide biphasic system, *J. Mol. Liq.* 218 (2016) 429–433.
- [21] A. Mahanta, M. Mondal, A.J. Thakur, U. Bora, An improved Suzuki–Miyaura cross-coupling reaction with the aid of in situ generated PdNPs: evidence for enhancing effect with biphasic system, *Tetrahedron Lett.* 57 (29) (2016) 3091–3095.
- [22] K.M.N. Borba, M.O. de Souza, R.F. de Souza, K. Bernardo-Gusmão, β-Diimine nickel complexes in BMI• AlCl₄ ionic liquid: a catalytic biphasic system for propylene oligomerization, *Appl Catal A-gen* 538 (2017) 51–58.
- [23] A. Behr, Z. Bayrak, G. Samli, D. Yildiz, V. Korkmaz, S. Peitz, G. Stochniol, Recycling and oligomerization Activity of Ni/Al catalyst in a biphasic system with ionic liquids, *Chem. Eng. Technol.* 40 (1) (2017) 196–204.
- [24] Z. Császár, J. Bakos, G. Farkas, Sulfonated Phosphine Ligands in the Ruthenium Catalyzed Biphasic Hydrogenation of Unsaturated Hydrocarbons, *Catal. Lett.* (2020) 1–8.
- [25] A. Joumaa, S. Chen, S. Vincendeau, F. Gayet, R. Poli, E. Manoury, Rhodium-catalyzed aqueous biphasic hydrogenation of alkenes with amphiphilic phosphine-containing core-shell polymers, *Mol. Catal.* 438 (2017) 267–271.
- [26] S. Weber, J. Brünig, V. Zeindlhofer, C. Schröder, B. Stöger, A. Limbeck, K. Kirchner, K. Bica, Selective Hydrogenation of Aldehydes Using a Well-Defined Fe (II) PNP Pincer Complex in Biphasic Medium, *ChemCatChem* 10 (19) (2018) 4386–4394.
- [27] M. Schmidt, T. Pogrzeba, L. Hohl, A. Weber, A. Kielholz, M. Kraume, R. Schomäcker, Palladium catalyzed methoxycarbonylation of 1-dodecene in biphasic systems—optimization of catalyst recycling, *Mol. Catal.* 439 (2017) 1–8.
- [28] F. Monteil, P. Kalck, Carbonylation of bromobenzene in a biphasic medium catalyzed by water-soluble palladium complexes derived from tris (3-sulphophenyl) phosphine, *J. Organomet. Chem.* 482 (1–2) (1994) 45–51.
- [29] R. Pruvost, J. Boulanger, B. Leger, A. Ponchel, E. Monflier, M. Ibert, A. Mortreux, M. Sauthier, Biphasic Palladium-Catalyzed Hydroesterification in a Polyol Phase: selective Synthesis of Derived Monoesters, *ChemSusChem* 8 (12) (2015) 2133–2137.
- [30] T. Gaide, A. Behr, M. Terhorst, A. Arns, F. Benski, A.J. Vorholt, Catalyst Comparison in the Hydroesterification of Methyl 10-Undecenoate in Thermomorphic Solvent Systems, *Chem. Ing. Tech.* 88 (1–2) (2016) 158–167.
- [31] A. Behr, A. Vorholt, N. Rentmeister, Recyclable homogeneous catalyst for the hydroesterification of methyl oleate in thermomorphic solvent systems, *Chem. Eng. Sci.* 99 (2013) 38–43.
- [32] T.A. Tshabalala, S.O. Ojwach, Tuning the regioselectivity of (benzimidazolylmethyl) amine palladium (II) complexes in the methoxycarbonylation of hexenes and octenes, *Transition Met. Chem.* 43 (4) (2018) 339–346.
- [33] T.A. Tshabalala, S.O. Ojwach, M.A. Akerman, Palladium complexes of (benzimidazol-2-ylmethyl) amine ligands as catalysts for methoxycarbonylation of olefins, *J. Mol. Catal. A: Chem.* 406 (2015) 178–184.
- [34] Z. Zulu, G.S. Nyamato, T.A. Tshabalala, S.O. Ojwach, Palladium (II) complexes of (pyridyl) imine ligands as catalysts for the methoxycarbonylation of olefins, *Inorg. Chim. Acta* 501 (2020) 119270.
- [35] M.G. Alam, T.A. Tshabalala, S.O. Ojwach, Metal-Catalyzed Alkene Functionalization Reactions Towards Production of Detergent and Surfactant Feedstocks, *J. Surfactants Deterg* 20 (1) (2017) 75–81.
- [36] S.O. Akiri, S.O. Ojwach, Methoxycarbonylation of olefins catalysed by homogeneous palladium (II) complexes of (phenoxy) imine ligands bearing alkoxy silane groups, *Inorg. Chim. Acta* 489 (2019) 236–243.
- [37] S. Zulu, M.G. Alam, S.O. Ojwach, M.P. Akerman, Structural and theoretical studies of the methoxycarbonylation of higher olefins catalysed by (Pyrazolyl-ethyl) pyridine palladium (II) complexes, *Appl. Organomet. Chem.* 33 (11) (2019) e5175.
- [38] S.O. Akiri, S.O. Ojwach, Synthesis of MCM-41 Immobilized (Phenoxy) Imine Palladium (II) Complexes as recyclable catalysts in the methoxycarbonylation of 1-hexene, *Catalysts* 9 (2) (2019) 143.
- [39] N. Kumari, V.K. Yadav, S. Zališ, L. Mishra, Pd (II) catalyzed transformation of Schiff bases in complexes of the type trans-[PdCl₂ (NH₂ 2 Ar-X) 2](X= H, CH₃, Cl): reactivity with aldehydes and Heck coupling reaction, *Indian J. Chem.* 51A (2012) 554–563.
- [40] B. APEXSAINT and SADABS, Bruker AXS Inc., Madison, Wisconsin, USA, 2010.
- [41] G.M. Sheldrick, Crystal structure refinement with SHELXL, *ACTA CRYSTALLOGR C* 71 (1) (2015) 3–8.
- [42] M. Botsivali, D.F. Evans, P.H. Missen, M.W. Upton, Studies on singlet oxygen in aqueous solution. Part 2. Water-soluble square-planar nickel complexes as quenchers, *J. Chem. Soc., Dalton Trans* (6) (1985) 1147–1149.
- [43] B. Choudary, T. Ramani, H. Maheswaran, L. Prashant, K. Ranganath, K.V. Kumar, Catalytic Asymmetric Epoxidation of Unfunctionalised Olefins using Silica, LDH and Resin-Supported Sulfonato-Mn (salen) Complex, *Adv. Synth. Catal.* 348 (4–5) (2006) 493–498.
- [44] C. Fasina, Synthesis, electronic spectra and inhibitory study of some Salicylaldehyde Schiff bases of 2-aminopyridine, *Afr. J. Pure Appl. Sci.* 5 (2) (2011) 13–18.
- [45] T. Stringer, P. Chellan, B. Therrien, N. Shunmoogam-Gounden, D.T. Hendricks, G.S. Smith, Synthesis and structural characterization of binuclear palladium (II) complexes of salicylaldehyde dithiosemicarbazones, *Polyhedron* 28 (14) (2009) 2839–2846.
- [46] P.A. Aguirre, C.A. Lagos, S.A. Moya, C. Zúñiga, C. Vera-Oyarce, E. Sola, G. Peris, J.C. Bayón, Methoxycarbonylation of olefins catalyzed by palladium complexes bearing P, N-donor ligands, *Dalton Trans.* (46) (2007) 5419–5426.
- [47] G. Cavinato, L. Toniolo, Carbonylation of ethene catalysed by Pd (II)-phosphine complexes, *Molecules* 19 (9) (2014) 15116–15161.
- [48] I. del Río, C. Claver, P.W. van Leeuwen, On the mechanism of the hydroxycarbonylation of styrene with palladium systems, *Eur. J. Inorg. Chem.* 2001 (11) (2001) 2719–2738.
- [49] C. Bianchini, A. Meli, W. Oberhauser, P.W. van Leeuwen, M.A. Zuideveld, Z. Freixa, P.C. Kamer, A.L. Spek, O.V. Gusev, A.M. Kal'sin, Methoxycarbonylation of Ethene by Palladium (II) Complexes with 1, 1'-Bis (diphenylphosphino) ferrocene (dppf) and 1, 1'-Bis (diphenylphosphino) octamethylferrocene (dp-pomf), *Organometallics* 22 (12) (2003) 2409–2421.
- [50] G. Kiss, Palladium-catalyzed Reppe carbonylation, *Chem. Rev.* 101 (11) (2001) 3435–3456.
- [51] C.-M. Tang, X.-L. Li, G.-Y. Wang, A highly efficient catalyst for direct synthesis of methyl acrylate via methoxycarbonylation of acetylene, *Korean J. Chem. Eng.* 29 (12) (2012) 1700–1707.
- [52] H.S. Yun, K.H. Lee, J.S. Lee, The regioselective hydrocarboalkoxylation of 4-methylstyrene catalyzed by palladium complexes, *J. Mol. Catal. A: Chem.* 95 (1) (1995) 11–17.
- [53] A. Seayad, A. Kelkar, L. Toniolo, R. Chaudhari, Hydroesterification of styrene using an in situ formed Pd (OTf)₂ (PPh₃)₂ complex catalyst, *J. Mol. Catal. A: Chem.* 151 (1–2) (2000) 47–59.
- [54] R. Bertania, G. Cavinato, L. Toniolo, G. Vasapollo, New alkoxy carbonyl complexes of palladium (II) and their role in carbonylation reactions carried out in the presence of an alcohol, *J. Mol. Catal.* 84 (2) (1993) 165–176.
- [55] C. Zuniga, D. Sierra, J. Oyarzo, A. Klahn, Methoxycarbonylation of styrene by palladium (II) complex containing the diphenylphosphinocyclohexene ligand, *Journal of the Chilean Chemical Society* 57 (2) (2012) 1101–1103.
- [56] F. Stempfle, D. Quinzler, I. Heckler, S. Mecking, Long-chain linear C19 and C23 monomers and polycondensates from unsaturated fatty acid esters, *Macromolecules* 44 (11) (2011) 4159–4166.
- [57] H.A. Ghaly, A.S. El-Kalliny, T.A. Gad-Allah, N.E.A. El-Sattar, E.R. Souaya, Stable plasmonic Ag/AgCl-polyaniline photoactive composite for degradation of organic contaminants under solar light, *RSC Adv* 7 (21) (2017) 12726–12736.
- [58] A.F. Schmidt, A. Al-Halalqa, V.V. Smirnov, Effect of macrokinetic factors on the ligand-free Heck reaction with non-activated bromoarenes, *J. Mol. Catal. A: Chem.* 250 (1–2) (2006) 131–137.

- [59] R.B. Bernstein, *Atom-molecule Collision theory: a Guide For the Experimentalist*, Springer Science & Business Media, 2013.
- [60] J.J. de Pater, D. Tromp, D.M. Tooke, A.L. Spek, B.-J. Deelman, G. van Koten, C.J. Elsevier, Palladium (0)-Alkene Bis (triarylphosphine) complexes as catalyst precursors for the methoxycarbonylation of styrene, *Organometallics* 24 (26) (2005) 6411–6419.
- [61] M.K. YILMAZ, S. İnce, Palladium (II) Complexes of Monodentate Phosphine Ligands and Their Application as Catalyst in Suzuki-Miyaura CC Coupling Reaction at Room Temperature, *J. Turkish chem. soc.* 5 (2) (2018) 895–902.
- [62] Z. Kokan, B. Perić, G. Kovačević, A. Brozovic, N. Metzler-Nolte, S.I. Kirin, cis-versus trans-Square-Planar Palladium (II) and Platinum (II) Complexes with Triphenylphosphine Amino Acid Bioconjugates, *Eur. J. Inorg. Chem.* 2017 (33) (2017) 3928–3937.
- [63] C. Blanco, C. Godard, E. Zangrando, A. Ruiz, C. Claver, Room temperature asymmetric Pd-catalyzed methoxycarbonylation of norbornene: highly selective catalysis and HP-NMR studies, *Dalton Trans* 41 (23) (2012) 6980–6991.
- [64] J.S. Kim, A. Sen, I.A. Guzei, L.M. Liable-Sands, A.L. Rheingold, Synthesis and reactivity of bimetallic palladium (II) methyl complexes with new functional phosphine ligands, *J. Chem. Soc., Dalton Trans.* (24) (2002) 4726–4731.
- [65] Y. Cabon, I. Reboule, M. Lutz, R.J. Klein Gebbink, B.-J. Deelman, Oxidative Addition of Sn–C Bonds on Palladium (0): identification of Palladium–Stannyl Species and a Facile Synthetic Route to Diphosphinostannylenes–Palladium Complexes, *Organometallics* 29 (22) (2010) 5904–5911.
- [66] J.H. Nelson, Aspects of equivalence as illustrated by phosphine complexes of transition metals, *Concepts in Magnetic Resonance, An Edu. J.* 14 (1) (2002) 19–78.
- [67] L. Crawford, D.J. Cole-Hamilton, M. Bühl, Uncovering the mechanism of homogeneous methyl methacrylate formation with p, n chelating ligands and palladium: favored reaction channels and selectivities, *Organometallics* 34 (2) (2015) 438–449.
- [68] P. Roesle, L. Caporaso, M. Schnitte, V. Goldbach, L. Cavallo, S. Mecking, A comprehensive mechanistic picture of the isomerizing alkoxy carbonylation of plant oils, *J. Am. Chem. Soc.* 136 (48) (2014) 16871–16881.
- [69] R.P. Tooze, K. Whiston, A.P. Malyan, M.J. Taylor, N.W. Wilson, Evidence for the hydride mechanism in the methoxycarbonylation of ethene catalysed by palladium–triphenylphosphine complexes, *J. Chem. Soc., Dalton Trans.* (19) (2000) 3441–3444.
- [70] G.R. Eastham, R.P. Tooze, M. Kilner, D.F. Foster, D.J. Cole-Hamilton, Deuterium labelling evidence for a hydride mechanism in the formation of methyl propanoate from carbon monoxide, ethene and methanol catalysed by a palladium complex, *J. Chem. Soc., Dalton Trans.* (8) (2002) 1613–1617.
- [71] G. Cavinato, A. Vavasori, L. Toniolo, F. Benetollo, Synthesis, characterization and X-ray structure of trans-[Pd (COOCH₃)₃(H₂O)(PPh₃)₂](TsO), a possible intermediate in the catalytic hydroesterification of olefins (TsO= p-toluenesulfonate), *Inorg. Chim. Acta* 343 (2003) 183–188.
- [72] R.E. Harmon, S. Gupta, D. Brown, Hydrogenation of organic compounds using homogeneous catalysts, *Chem. Rev.* 73 (1) (1973) 21–52.
- [73] S.B. Dake, R.V. Chaudhari, Solubility of carbon monoxide in aqueous mixtures of methanol, acetic acid, ethanol and propionic acid, *J. Chem. Eng. Data* 30 (4) (1985) 400–403.
- [74] R. Sang, P. Kucmierczyk, R. Dühren, R. Razzaq, K. Dong, J. Liu, R. Franke, R. Jackstell, M. Beller, Synthesis of Carboxylic Acids by Palladium-Catalyzed Hydroxycarbonylation, *Angew. Chem. Int. Ed.* 58 (40) (2019) 14365–14373.
- [75] B. Richter, A.L. Spek, G. van Koten, B.-J. Deelman, Fluorous versions of Wilkinson's catalyst. Activity in fluorous hydrogenation of 1-alkenes and recycling by fluorous biphasic separation, *J. Am. Chem. Soc.* 122 (16) (2000) 3945–3951.
- [76] J. Dupont, P.A. Suarez, A.P. Umpierre, R.F.d. Souza, Pd (II)-dissolved in ionic liquids: a recyclable catalytic system for the selective biphasic hydrogenation of dienes to monoenes, *J. Braz. Chem. Soc.* 11 (3) (2000) 293–297.